Preprints of the 21st IFAC World Congress (Virtual)
Berlin, Germany, July 12-17, 2020

Application of Model-based Online Monitoring and Robust Optimizing Control to Fed-Batch Bioprocesses

Rubin Hille*, Heiko Brandt*, Vera Colditz*, Jens Classen, Lukas Hebing*, Matthäus Langer**, Steffen Kreye**, Tobias Neymann*,(†), Stefan Krämer*,***, Jens Tränkle**, Helmut Brod**, Alexander Jockwer****

** Engineering & Technology, Bayer AG, D-51373 Leverkusen, Germany*
*** Pharmaceuticals, Bayer AG, D-51373 Leverkusen, Germany*
**** Department of Biochemical and Chemical Engineering, TU Dortmund, D-44221 Dortmund, Germany*
(†) deceased in July 2018

Abstract: The aim of the quality by design initiative is to assure a continuous and high-quality production of pharmaceuticals despite the presence of process variations and disturbances. This need for optimal process operation necessitates the use of accurate prediction and fault detection methods in combination with advanced control strategies. However, the critical component for the success of such an approach is a mathematical model providing an adequate representation of the bioprocess under study. This work presents a framework for bioprocess online optimization that utilizes rigorous modelling and control methods tailored for fed-batch and perfusion cultures. The basis of the methodology is a hybrid process modelling approach which enables both monitoring and optimization of cell culture processes. To account for inherent process variability of biological organisms, an adaptive state estimation approach is utilized which employs multiple models in parallel thus providing improved robustness to a possible occurrence of model-plant mismatch. Furthermore, optimal process trajectories for online optimization are calculated using a robust multistage nonlinear model predictive control approach which considers different scenarios based on the employed process models. Recent promising results from experimental fed-batch CHO fermentations are presented which show significant productivity increases.

Keywords: Fed-Batch, Bioprocess, Adaptive State Estimation, Optimizing Control, Multi-Stage MPC

1. INTRODUCTION

Due to their complex behaviour and characteristic variability, cell culture processes present a challenging environment for the utilization of predictive methods. The quality by design (QbD) initiative from the Food and Drug Administration (FDA) for the production of biopharmaceuticals therefore necessitates advanced monitoring and control capabilities that provide the required robustness and flexibility. This work presents recent extensions and application of a framework for the development of a hybrid bioprocess model, adaptive state-estimation and robust model predictive control tailored for the online optimization of fed-batch processes.

The basis of an effective QbD approach for biopharmaceuticals is provided by an adequate model of the process under study. In this work, we are interested in the optimization of Chinese hamster ovary (CHO) cultures for which the development of mechanistic models presents an active research area (Yahia *et al.*, 2015). To describe the dynamic behaviour of cells during fermentation, a modelling methodology (Provost *et al.*, 2006) is used which broadly aims at obtaining specific macro reactions that provide a significant contribution to the observed uptake and production rates of the major metabolites. Using these macro reactions, it is possible to automatically generate kinetics (Hebing *et al.*, 2016) that allow for a mechanistic description of the dynamics of major metabolites during the fermentation process. To derive models that are tailored for process optimization it is further necessary to explore the space of bioprocess parameters, e.g. dissolved oxygen (DO), stirrer speed, pH and temperature regimes, to determine their effect on the cell metabolism. By augmenting the mechanistic model with empirical structures, it is possible include these observed effects to generate a so-called hybrid process model which subsequently can be used for process optimization.

However, given the complex nature of organisms, an online application of a process model requires monitoring techniques that provide robustness and flexibility in order to deal with a changing environment. In that regard, it is possible to utilize state estimators such as Kalman filters (Gelb 1988; Ohadi *et al.*, 2015) to obtain more accurate estimates of the bioprocess states in the presence of noisy measurements. For additional robustness against model-plant mismatch Hebing *et al.* (2020a) proposed an adaptive constrained extended Kalman filter (CEKF) where the most suitable model is selected based on a trust-index. Regarding the implementation of an advanced process control scheme, we applied a robust multi-stage non-linear model predictive controller (RS-NMPC) (Lucia *et al.*, 2013) on a shrinking horizon where, in each iteration, an optimization problem is solved in order to determine the optimal trajectory of manipulated process parameters for the remaining days of the fermentation. The multi-stage MPC approach allows for the accounting of uncertainty by considering different models as branches in a scenario tree.

In the experimental study, we used the advanced control scheme to achieve two objectives. The first goal was to perform set-point tracking of the glucose concentration inside the bioreactor. In this case, a precise regulation was achieved with the help of a Raman probe which provides frequent measurements thus enabling a more effective feedback control. The second goal was to maximize the amount of obtained product at the end of the fed-batch duration. This was accomplished by optimizing a set of process parameters throughout the cultivation. Experimental fed-batch runs were realized using 10 L glass reactors where several reactors were optimized using the proposed advanced monitoring and control strategy while the remaining reactors served as the control group that were operated following standard operating procedure.

2. BIOPROCESS MODEL

In the following, we will present a brief outline of the development of a dynamic metabolic model of a bioprocess which can be utilized for monitoring and optimization purposes.

A typical representation of a component i in a fed-batch bioprocess is given by:

$$\frac{dc_i}{dt} = D \cdot \left(c_{i,in} - c_i\right) + \boldsymbol{L}_i^T \cdot \boldsymbol{r} \cdot X_v \tag{1}$$

where $c_{i,in}$ denotes the concentration of component i in the feed, D the dilution rate, $\boldsymbol{L}_i$ a set of macro-reactions related to component i, $\boldsymbol{r}$ the vector of corresponding cell-specific reaction rates and X_v the viable cell density. Given a known network of intra-cellular reactions, the first step of the model development is to determine the set of significant reactions that make up the matrix of macro-reactions $\boldsymbol{L}$. Based on experimental data, it is possible to calculate cell-specific uptake and production rates of each of the metabolites (Hebing *et al*., 2020b). These are required to subsequently determine which intra-cellular reactions are of significant magnitude in order explain the observed data. Using the determined rates, it is then possible to construct so-called elementary modes (EMs) which describe direct intra-cellular pathways between substrates and products (Provost *et al*., 2006). As the number of feasible elementary modes can be quite large, we are interested in a minimal set of modes that are able to explain the given data. To accomplish this task, a multi-objective optimization is performed according to Hebing *et al*. (2016) with the goal of finding an optimal trade-off between accuracy and complexity by selecting the cut-off value in terms of number of EMs such that we still obtain a satisfactory prediction of the observed concentration profiles. Based on the derived minimal set of modes, we notice that by a linear combination of EMs we obtain the matrix of macro-reactions $\boldsymbol{L}$ that is relating the formation of each metabolite to a consumption of another metabolite. Having obtained matrix $\boldsymbol{L}$, as required in (1), we are subsequently interested in the construction of the kinetic expressions $\boldsymbol{r}$ that govern the dynamics of the cell cultivation process.

1.1 Reaction Rate Kinetics

In general, a reaction rate j that involves limiting or inhibiting substrates can be described as follows:

$$\begin{aligned} r_j &= f_{\text{kinetic}}(\boldsymbol{c},\boldsymbol{z}) \\ &= r_{j,\max} \cdot \prod_{i=1}^{n_t} \tilde{r}_{j,i}^{lim}(\boldsymbol{c}) \cdot \tilde{r}_{j,i}^{inhib}(\boldsymbol{c}) \cdot \prod_{k=1}^{n_z} \tilde{r}_{j,k}^{ker}(\boldsymbol{z}) \end{aligned} \tag{2}$$

where $r_{j,\max}$ presents the maximum reaction rate, whereas $\tilde{r}_{j,i}^{lim}$ denotes a limiting kinetic while $\tilde{r}_{j,i}^{inhib}$ describes an inhibiting kinetic term related to substrate i with n_t being the number of substrates involved in the reaction. $\boldsymbol{c}$ denotes the vector of component concentrations. Furthermore, $\tilde{r}_{j,k}^{ker}$ present terms based on experimentally observed effects of operating conditions $\boldsymbol{z}$ on specific rates. Bioprocess specific operating conditions $\boldsymbol{z}$ include parameters such as DO, pH, temperature or impeller speed.

Substrate limitation kinetics of biochemical reactions can generally be described using Monod-kinetics:

$$\tilde{r}_{j,i}^{lim} = \left(\frac{c_i}{K_{m,j,i} + c_i}\right)^n \tag{3}$$

where c_i is the concentration of the limiting substrate and $K_{m,j,i}$ the Monod constant, whereas substrate inhibitions are given by Haldane kinetics:

$$\tilde{r}_{j,i}^{inhib} = \left(\frac{K_{I,j,i}}{K_{I,j,i} + c_i}\right)^n \tag{4}$$

where $K_{I,j,i}$ presents the inhibition constant. Thus, assuming Monod or Haldane kinetics in each of the resulting macro-reactions, it is possible to generate a set of ordinary differential equations according to (1) that represent the dynamic behaviour of the process under study.

1.2 Hybrid Model Structures

Using (2) - (4) it is possible to semi-mechanistically characterize biochemical reaction rates that involve the concentrations of limiting or inhibiting substrates. However, the effect of operating conditions $\boldsymbol{z}$ on certain reaction rates are of vital importance for optimization purposes and can be represented by empirical structures. Similar to the Monod kinetics (3), which change between zero-order and first-order dynamics, we want the effect of process conditions $\boldsymbol{z}$ on the affected reaction rates to be normalized between 0 and 1. Thus, the next step is to select a candidate model function which can best represent the phenomena, observed in experimental data. In this work, we select a multivariate distribution to model the influence of $\boldsymbol{z}$ on the different specific uptake and production rates. This distribution, also referred to as kernel, is given as follows:

$$\tilde{r}_{j,k}^{ker} = \exp\left(-\frac{1}{2}(\boldsymbol{z}_k - \boldsymbol{\mu}_k)^T \boldsymbol{\Sigma}_k^{-1} (\boldsymbol{z}_k - \boldsymbol{\mu}_k)\right) \tag{5}$$

where $\boldsymbol{z}_k$ denotes a subset of process conditions while $\boldsymbol{\mu}_k$ and $\boldsymbol{\Sigma}_k$ represent kernel tuning parameters that need to be estimated from experimental data. Using the approach of obtaining a semi-mechanistic model structure based on known intracellular reactions and then augmenting the rates (2) with influences of additional process parameters (5) thus leads to a hybrid bioprocess model.

1.3 Optimizing Inputs

The available bioprocess operating condition variables $\boldsymbol{z}$ can be used for optimization purposes if they were found to affect rates of interest such as the growth rate or specific productivity. For the remainder of the paper, the subset of operating conditions whose set-points can be manipulated for optimization purposes are defined as:

$$\boldsymbol{u}_{opt} \subseteq \boldsymbol{z} \tag{6}$$

3. STATE ESTMATION

The complex nature of bioprocesses presents a challenge for monitoring and control applications due to large changes in concentrations during fermentation and sparse sampling of metabolites that are typically taken only once per day. In order to maintain an accurate estimation of the relevant states during the fermentation, it is therefore vital to employ state estimators. As stated in (1), a process model can be generally expressed as a system of ODEs as follows:

$$\dot{\boldsymbol{x}} = \mathrm{f}(\boldsymbol{x}, \boldsymbol{\theta}, \boldsymbol{u}, \boldsymbol{z}) + \boldsymbol{\nu} \tag{7}$$

$$\boldsymbol{y} = \mathrm{h}(\boldsymbol{x}) + \boldsymbol{\eta} \tag{8}$$

where $\boldsymbol{x}$ represent the state variables, $\boldsymbol{\theta}$ a set of model parameters, $\boldsymbol{u}$ the vector of model inputs and $\boldsymbol{y}$ the model outputs. Moreover, $\boldsymbol{\nu}$ presents the measure of process noise whereas $\boldsymbol{\eta}$ quantifies the measurement noise. Typically, we assume these errors to be normally distributed with zero mean:

$$\boldsymbol{\nu} \sim \mathcal{N}(\boldsymbol{0}, \boldsymbol{Q}_k) \tag{9}$$

$$\boldsymbol{\eta} \sim \mathcal{N}(\boldsymbol{0}, \boldsymbol{R}_k) \tag{10}$$

where $\boldsymbol{Q}_k$ and $\boldsymbol{R}_k$ are the respective state noise covariance and measurement noise covariance matrices. In this work, we utilize an adaptive constrained extended Kalman filter (CEKF) (Hebing *et al.*, 2020a) to update the model states (7) based on online measurements from bioreactor sensors as well as measurements from analysed samples. To adapt the model to a varying environment and to counteract a possible occurrence of model-plant mismatch, adaptive correction factors are introduced as additional pseudo-states into important reactions rates (2) as follows:

$$r_j = f_{\text{kinetic}}(\boldsymbol{c}, \boldsymbol{z}) \cdot \delta_j \tag{11}$$

$$\frac{d\delta_j}{dt} = 0 \tag{12}$$

With an initial state value of $\delta_j(0) = 1$. The update of the correction factor is based on the observed mismatch between the model prediction and measured quantity and depends on the magnitude of process noise $\boldsymbol{Q}_k$. In addition to the adaptive correction factors, the implemented state estimation algorithm incorporates a multi-model architecture that selects the active model based on a trust-index. Accordingly, whenever a new measurement becomes available, the quality of each model j is evaluated based on the error between prediction and measurement as follows:

$$WSSR_k^j = \left(\mathrm{h}(\hat{\boldsymbol{x}}_{k,j}^-) - \boldsymbol{y}_k\right)^T \boldsymbol{R}_k^{-1} \left(\mathrm{h}(\hat{\boldsymbol{x}}_{k,j}^-) - \boldsymbol{y}_k\right) \tag{13}$$

where $\hat{\boldsymbol{x}}_{k,j}^-$ presents the *a-priori* estimate of the model states (7) at iteration k, while $\boldsymbol{y}_k$ denotes the respective process measurement. Furthermore, the error is weighted by the measurement covariance matrix $\boldsymbol{R}_k$. Based on the prediction error (13), the trust-index of each model is calculated as follows:

$$\varphi_k^j = \frac{\sum_j WSSR_k^j}{WSSR_k^j} \tag{14}$$

To prevent oscillations of active models between iterations, the trust-index in (14) is further processed by a first-order filter. Accordingly, in each estimation step, the model with the largest filtered trust-index is selected as the active model and thus used as basis for the subsequent optimization step.

4. OPTIMIZING CONTROL

Following the multi-model state estimation approach, we utilize a multi-stage NMPC approach (Lucia *et al.*, 2013) for calculating optimal trajectories of process inputs $\boldsymbol{u}$. Based on the trust-index (14) we define the current bioprocess states of the active model as $\hat{\boldsymbol{x}}_0^{am}$. As depicted in Fig. 1, using this set of states and the set of model specific parameters $\boldsymbol{\theta}_0^j$ as initial conditions, we can calculate, for each model j, the process evolution based on inputs $\boldsymbol{u}_k^j \; \forall \, k = 0, \ldots, n_p$, where n_p denotes the prediction horizon. Using the scenario representation as shown in Fig. 1, we can combine, for each model j, all future states and inputs as follows:

$$X_j = \left\{\boldsymbol{x}_0^j, \ldots, \boldsymbol{x}_{n_p}^j\right\} \tag{15}$$

$$U_j = \left\{\boldsymbol{u}_0^j, \ldots, \boldsymbol{u}_{n_p}^j\right\} \tag{16}$$

In each iteration of the NMPC optimization routine, the multi-stage approach is then solving the following problem (Hebing *et al.*, 2020a):

$$\begin{aligned} \min_{\boldsymbol{u}_k^j \in U_j} \; & \sum_{j=1}^{n_s} w_j \cdot \Phi\left(X_j, U_j\right) \\ \text{s.t.} \quad & \boldsymbol{u}_0^j = \boldsymbol{u}_0^l \qquad \forall j, l = 1, \ldots, n_s \\ & \boldsymbol{u}_{lb} \le \boldsymbol{u}_k^j \le \boldsymbol{u}_{ub} \qquad \forall \boldsymbol{u}_k^j \in U_j \\ & g\left(X_j\right) \le 0 \qquad \forall j = 1, \ldots, n_s \end{aligned} \tag{17}$$

where w_j presents the respective probability weight given to model j while n_s describes the total number of considered scenarios. $\boldsymbol{u}_{lb}$ and $\boldsymbol{u}_{ub}$ are lower and upper bounds on the input space whereas $g(X_j)$ presents process dependent constraints on future model states.

When the tracking of a desired concentration set-point of certain metabolites, e.g. glucose, is of interest, the objective function in (17) can be defined as follows:

$$\Phi_{tr} = \sum_{k=1}^{n_p-1} \boldsymbol{K}_{sp}^T \|\boldsymbol{y}_k - \boldsymbol{y}_{sp}\|^2 + \frac{\boldsymbol{K}_{\Delta u}^T}{\Delta t} \|\boldsymbol{u}_{k-1} - \boldsymbol{u}_k\|^2 \qquad (18)$$

Where $\boldsymbol{K}_{sp}$ and $\boldsymbol{K}_{\Delta u}$ presents weights on set-point errors and input changes respectively.

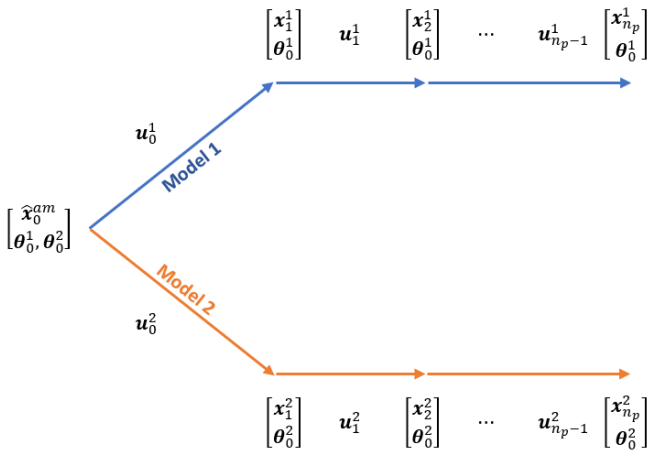

Fig. 1: Multi-stage NMPC scenario tree (adapted from Hebing *et al.* (2020a)).

Regarding the optimization of bioprocesses, the objective function Φ generally involves some growth or productivity measure. Therefore, when employing a short prediction horizon of $n_p = 3$ days, it is necessary to introduce a weighted objective between growth and productivity as proposed in Hebing *et al.* (2020a). This is essential to enable conditions for cell proliferation during the initial growth phase before switching to conditions that favor productivity but may stunt cell growth. However, from practical experience we found out that such a weighted objective increases complexity and is difficult to tune. In contrast to a weighted objective, in this work, we instead propose the use of a shrinking horizon implementation, where the horizon always covers the final batch time. Thus, we get for the prediction horizon:

$$n_p(i) = n_p(i-1) - 1, \quad n_p(0) = n_d \qquad (19)$$

where i represents the iteration index and n_d the number of fermentation days, i.e. $n_d = 14$. The shrinking horizon approach has the advantage that growth is implicitly considered as large cell densities are desired in order to obtain the maximum amount product at the end of the fed-batch. Thus, in terms of productivity optimization, the objective function used in (17) is defined as follows:

$$\Phi_{prod} = x_{n_p}^{prod}(X,U) + \frac{\boldsymbol{K}_{\Delta u}^T}{\Delta t} \sum_{k=1}^{n_p-1} \|\boldsymbol{u}_{k-1} - \boldsymbol{u}_k\|^2 \qquad (20)$$

where $x_{n_p}^{prod}$ denotes the product concentration at the end of the prediction horizon, which, following the shrinking horizon approach (19), is equal to the final batch time.

5. EXPERIMENTAL SET-UP

As mentioned in the Introduction, the control strategy of the experimental test run for optimizing the CHO cell fermentation process consists of two goals:

- Set-point tracking of the glucose concentration inside the bioreactor with use of a Raman probe
- Product maximization regarding a recombinant protein produced by the CHO cells

To pursue these two targets, we opted for the control structure illustrated in Fig. 2, where we distributed the two control problems into separate control systems. Control system #1 implemented the desired glucose pump settings $\boldsymbol{u}_{Glc}$ every 1 h, while control system #2 re-optimized yield related inputs $\boldsymbol{u}_{opt}$ with a frequency of 24 h. Using a 10 L glass bioreactor for fermentation, we were able to obtain analytical sample measurements of the metabolite concentrations $\boldsymbol{y}$ every 24 h while the bioreactor sensors provided online measurements of process conditions $\boldsymbol{z}$, e.g. pump rates, temperature, etc.

Using a Raman probe, it was possible to generate additional measurements of certain metabolites such as glucose at much faster rate compared to an offline sample analysis. The more frequent feedback signal from the Raman probe thus enabled us to perform a set-point tracking of the glucose concentration using control system #1 as shown in Fig. 2. For this experiment, we opted to control the glucose concentration around a pre-determined constant set-point. An adaptive CEKF, employing two parallel models, was used for state estimation as described in section 3. An RS-NMPC with a tracking objective function according to (18) was utilized to compute the glucose pump rates every 1 h. In this case, we selected a non-shrinking prediction and control horizon of $n_p = 3$ days. Finally, the optimal pump trajectories $\boldsymbol{u}_{Glc}^*$ were passed on to a distributed control system (DCU) which included an interface to the glucose pump.

For the more important goal, the maximization of obtained product at the end of the fed-batch, the second control system was utilized for optimizing growth and productivity during the fermentation. In this case, the process inputs considered most effective for optimization $\boldsymbol{u}_{opt}^*$ were used as the manipulated variables in the objective in (20). Compared to the set-point tracking controller, new input trajectories were calculated by the economic RS-NMPC only every 24h. Furthermore, to avoid any weighted trade-off between a growth and productivity objective, the shrinking horizon according to (19) was implemented.

Finally, to compare and validate any results from the advanced control set-up shown in Fig. 2, a set of reference reactors were run in parallel. The reference reactors were run as per a standard operating procedure which consisted of fixed standard set-points for process operating conditions, i.e. $T_{sp} = 36.5\,°C$, $pH_{sp} = 7$ and $DO_{sp} = 40\,\%$, as well as a daily bolus feeding of glucose.

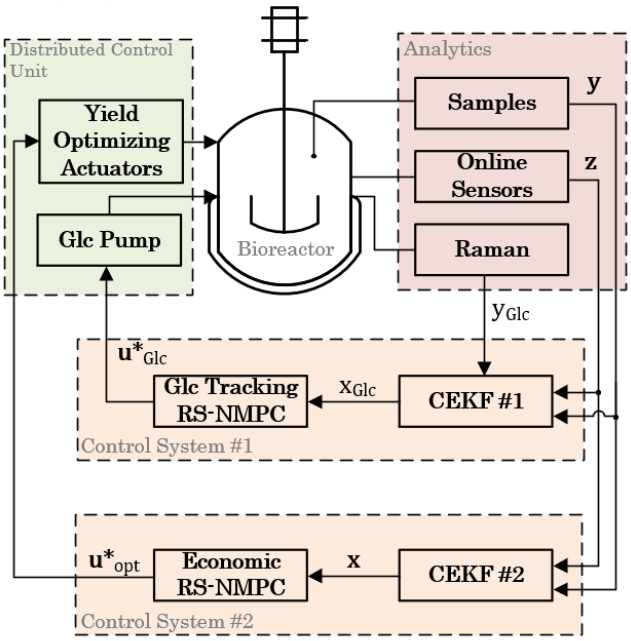

Fig. 2: Experimental control structure set-up used for glucose set-point tracking and product maximization.

6. RESULTS AND DISCUSSION

This section illustrates the results of the implemented control strategy to a CHO fed-batch cultivation with a duration of 14 days. Two dynamic metabolic models with different sets of parameters were used in each of the CEKFs depicted in Fig. 2. The models describe the dynamics of the major metabolites including viable and dead cell densities according to the derived macro-reactions. In addition, effects of various process conditions on specific rates of interest were incorporated using the kernel densities as stated in (5).

3.1 State Estimation

Using the adaptive CEKF described in section 3, we were able to obtain an online state estimation of the cell density and the remaining major metabolites during the fermentation. In terms of viable cell density, the performance of the state estimation, including the model prediction between samples, is illustrated in Fig. 3. A sample from the bioreactor was taken every 24h and the subsequent cell count used to get a measurement of the cell density. This measurement in turn was used to correct for any error in the model prediction. From Fig. 3 it is evident that the two models provide an accurate prediction of cell growth during the exponential phase. The prediction is less accurate during the cell density peak and the following post-exponential phase which lead to greater corrections from the state estimator.

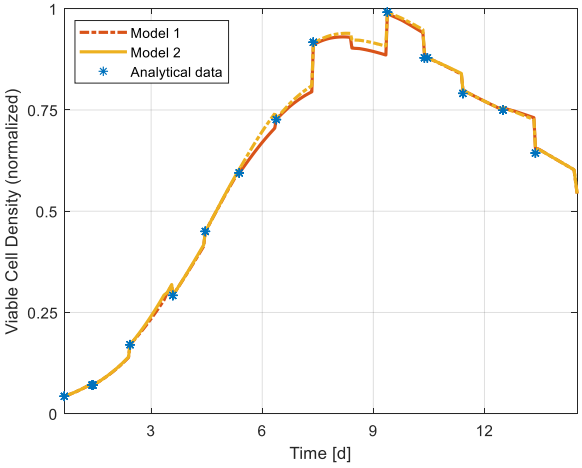

Fig. 3: State estimation of viable cell density during the fed-batch cultivation.

3.2 Glucose Set-Point Tracking

Using Raman probes to frequently infer the glucose concentration inside the bioreactor, it was possible to implement the glucose set-point control scheme using control system #1 as illustrated in Fig. 2. Fig. 4 depicts the glucose state estimation and set-point tracking performance during the first days of the cultivation.

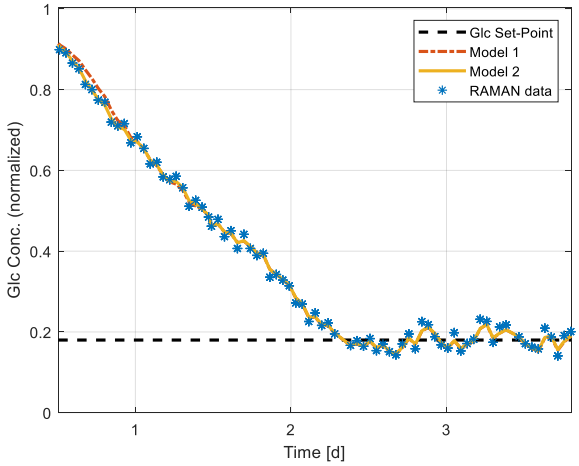

Fig. 4: Performance of the glucose set-point tracking controller (results are normalized).

First, it can be observed that the two models start out with slightly different glucose consumption dynamics. However, due to the use of the correction factors as outlined in (11) and (12), the cell-specific glucose consumption rate was quickly adapted to match the one observed from the Raman measurements. In the initial phase of a fed-batch process, the cells are consuming the glucose provided by the initial amount of medium, thus leading to a decrease in the concentration over time. Once the desired set-point is reached, fresh glucose was provided based on the controller output via a glucose pump. From Fig. 4 it is clear that, by using the Raman signal with a frequency of ~1h as feedback, it is possible to achieve an excellent set-point tracking of a metabolite inside the bioreactor.

3.3 Optimizing Control

While control system #1 was designed to keep the glucose concentration at the desired set-point, the purpose of control system #2 was to optimize the growth and productivity conditions as to maximize the amount of product at the end of the fed-batch. For that reason, the set of inputs $\boldsymbol{u}_{opt}$ was adjusted over the course of the cultivation according the model-based objective provided in (20). Fig. 5 illustrates the implemented trajectory of inputs $u_{opt,1}$ and $u_{opt,2}$ during the fermentation. In addition, it is possible to illustrate the process operating regions that, according to the estimated kernels (5), favour growth and productivity respectively. Fig. 5 shows that the shrinking horizon approach implicitly promotes cell growth during the initial growth phase of the fed-batch while facilitating productivity during the later stages when the cells are shifting to a post-exponential phase.

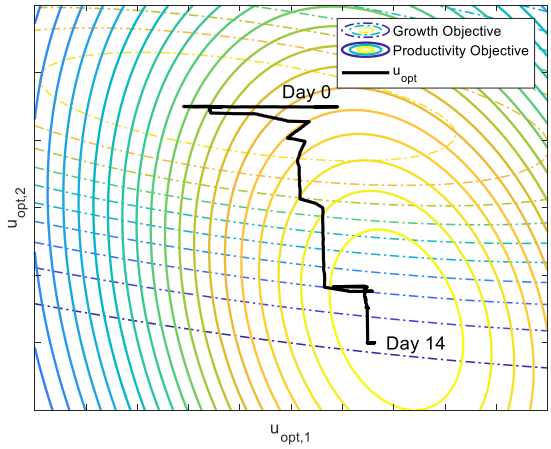

Figure 5: Optimal implemented trajectory of the inputs used for process optimization.

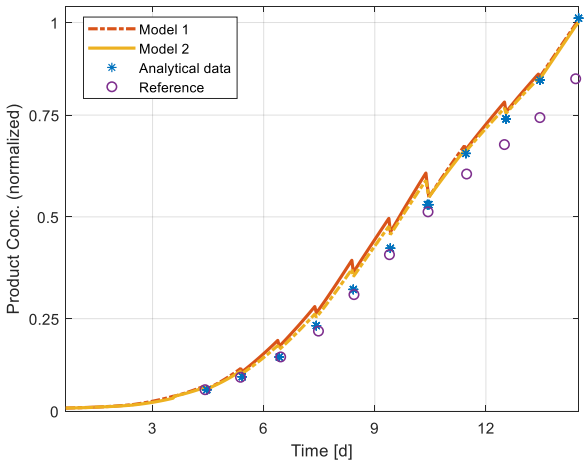

Figure 6: Product concentration over the course of fermentation. Comparison with reference reactor.

The main goal of the optimal input trajectory, illustrated in Fig. 5, is an increase the amount of product obtained at the end of the fed-batch cultivation. In this regard, Fig. 6 compares the performance of a bioreactor using the optimizing control strategy with a reference reactor which was operated according to standard operating procedure. It is evident that by optimizing the process conditions during fermentation, it is possible to achieve an increase in productivity of ca. 20% compared to a standard fed-batch operating strategy. These improvements present very promising results and show that advanced model-based optimizing control strategies offer the potential of automating bioprocess operation as well as enhancing yields.

7. CONCLUSIONS

This contribution presents the application of a framework for modelling, estimation and control of bioprocesses. An adaptive CEKF is utilized for obtaining accurate metabolite concentration during cultivation using dynamic metabolic models for prediction in between samples. Furthermore, using an RS-NMPC approach, a successful set-point tracking of the glucose concentration inside the bioreactor was achieved by using frequent Raman measurements. Finally, by implementing an optimizing control strategy it was possible to realize a significant improvement in the amount of recombinant proteins at the end of the fed-batch cultivation. Overall these promising results show a successful application of advanced and robust control strategies to bioprocesses.

REFERENCES

Gelb, A. (1988). Applied Optimal Estimation. Cambridge, MA, MIT Press.

Hebing, L., Neymann, T., Thüte, T., Jockwer, A., and Engell, S. (2016). Efficient generation of models of fed-batch fermentations for process design and control. DYCOPS, 621-626.

Hebing, L., Tran, F., Brandt, H., and Engell, S. (2020a). Robust optimizing control of fermentation processes based on a set of structurally different process models. *Ind Chem Eng*, 59, 2566-2580.

Hebing, L., Neymann, T., and Engell, S. (2020b). Application of dynamic metabolic flux analysis for process modeling: robust flux estimation with regularization, confidence bounds and selection of elementary modes. *Biotechnol Bioeng*, [accepted].

Lucia, S., Finkler, T., and Engell, S. (2013). Multi-stage nonlinear model predictive control applied to a semi-batch polymerization reactor under uncertainty. *J Proc Contr*, 1306-1319.

Ohadi, K., Legge, R.L., and Budman, H. (2015). Development of a soft-sensor based on multi-wavelength fluorescence spectroscopy and a dynamic metabolic model for monitoring mammalian cell cultures. *Biotechnol Bioeng*, 112, 197-208.

Provost, A., Bastin, G., Agathos, S. N., and Schneider, Y. J. (2006). Metabolic design of macroscopic bioreaction models: application to chinese hamster ovary cells. *Bioprocess Biosystems Eng*, 29, 349–366.

Yahia, B. B., Malphettes, L., and Heinzle, E. (2015). Macroscopic modeling of mammalian cell growth and metabolism. *Appl Microbiol Biotechnol*, 99, 7009–7024.